Convergence Analysis of the Modified Frequency Domain Block LMS Algorithm with Guaranteed Optimal Steady State Performance

Jing Lu, Kai Chen and Xiaojun Qiu

Abstract — The well-known bin-normalized frequency domain block LMS (NFBLMS) algorithm, although theoretically having very fast convergence speed, suffers from convergence to a biased steady state solution when the reference signal lags behind the desired signal or the adaptive filter is of deficient length. A modified FBLMS (MFBLMS) algorithm has been proposed with guaranteed optimal steady state performance at the cost of only one more FFT/IFFT pair. In this paper, the convergence behavior of the MFBLMS algorithm is analyzed using the theory of asymptotical equivalent matrices, and a theoretical eigenvalue spread is provided based on the first-order autoregressive (AR) model. It is found that the eigenvalues of the matrix controlling the convergence behavior have the tendency to be equally distributed, therefore the convergence speed of the MFBLMS is significantly higher than that of the time domain LMS algorithm for colored reference signal. Simulations are carried out to validate the convergence behavior predicted from the theoretical analysis.

Index Terms—Adaptive filters, Frequency-domain implementation, Eigenvalue distribution, Convergence behavior

I. INTRODUCTION

The frequency domain block least mean square (FBLMS) algorithm is a computational efficient implementation of the block LMS (BLMS) algorithm [1,2]. The computational complexity of the FBLMS algorithm is significantly less than that of the time domain LMS algorithm because the fast Fourier transform (FFT) is used to calculate both the block filtering output and the update terms in frequency domain. Furthermore, when the step size of the adaptive filter

Manuscript received May 30, 2016. This work was supported by the National Science Foundation of China No. 11374156 and No. 11474163.
The first two authors are with the Key Lab of Modern Acoustics (MOE), Institute of Acoustics, Nanjing University, Nanjing 210093, China, and the last author is with Faculty of Engineering and Information Technology, University of Technology Sydney, NSW 2007, Australia. (e-mail: lujing@nju.edu.cn, chenkai@nju.edu.cn, xiaojun.qiu@uts.edu.au).

is normalized by the reference signal power in each frequency bin, the convergence speed of the normalized FBLMS (NFBLMS) algorithm can be significantly increased for reference signals with large power spectra disparity. Theoretically it has been proven that the NFBLMS algorithm is capable of equalizing all modes of convergence [1]. Optimization of the stepsize in each frequency bin has also been further discussed by several researchers [3-5]. Due to the above advantages, the NFBLMS algorithm is widely used in many applications that require both large filter length and fast convergence speed, e.g, acoustic echo cancellation, active noise control, channel estimation and equalizations [6-8].

Although the NFBLMS algorithm has the significant merits of low computational complexity and fast convergence speed, its steady state value of the mean square error has been found to be increased in non-causal circumstances [9] and/or with deficient filter length [10]. An efficient modification of the NFBLMS algorithm, named as the MFBLMS algorithm has been proposed, which can guarantee the optimal steady state behavior with limited extra computational burden of one more FFT/IFFT pair [11]. The optimal steady state behavior of the MFBLMS algorithm has been demonstrated in the simulations in the reference, but its convergence behavior has not analyzed.

This paper investigates the convergence property of the MFBLMS algorithm by using the theory of asymptotical equivalent matrices [12]. The first-order AR models are utilized to establish a theoretical eigenvalue spread of the algorithm, and the eigenvalues of the matrix controlling the convergence behavior are found to have the tendency to be equally distributed as that of an identity matrix, an indication of a good convergence behavior. Please claim the significance and potential impact of the new contribution? The method for understanding the convergence behavior can be used in broader areas? Better performance is obtained with the method and understanding?

Throughout this paper, lower case letters are used for scalar quantities, bold lowercase for vectors and bold uppercase for matrices. Subscript "*f*" denotes frequency domain representation of each signal and "*k*" is reserved for the block index.

II. Analysis of Convergence Behavior

A. Review of the NFBLMS and MFBLMS algorithms

Let $\boldsymbol{x}(k) = [x(kN\text{-}N), x(kN\text{-}N+1), \ldots, x(kN+N\text{-}1)]^{\mathrm{T}}$ be the reference signal vector, where the superscript T represents the transpose operation, $\boldsymbol{w}(k) = [w_0(k), w_1(k), \ldots, w_{N\text{-}1}(k)]^{\mathrm{T}}$ be the N-tap finite impulse response (FIR) filter, and $\boldsymbol{d}(k) =$

$[d(kN\text{-}N), d(kN\text{-}N+1), \ldots, d(kN+N\text{-}1)]^{\mathrm{T}}$ be the desired signal vector, then the error vector in frequency domain can be described as

$$\mathbf{e}_f(k) = \mathbf{F}\mathbf{G}_{0,N}\mathbf{F}^{-1}\left[\mathbf{d}_f(k) - \mathbf{X}_f(k)\mathbf{w}_f(k)\right], \tag{1}$$

where $\mathbf{F}$ represents a $2N\times2N$ discrete Fourier transform (DFT) matrix, $\mathbf{d}_f(k) = \mathbf{F}[\mathbf{0}_{1\times N}, \mathbf{d}^{\mathrm{T}}(k)]^{\mathrm{T}}$, $\mathbf{X}_f(k) = \mathrm{diag}[\boldsymbol{x}_f(k)] = \mathrm{diag}[\mathbf{F}\boldsymbol{x}(k)]$, $\mathbf{w}_f(k) = \mathbf{F}[w^{\mathrm{T}}(k), \mathbf{0}_{1\times N}]^{\mathrm{T}}$ and

$$\mathbf{G}_{0,N} = \begin{bmatrix} \mathbf{0}_{N\times N} & \mathbf{0}_{N\times N} \\ \mathbf{0}_{N\times N} & \mathbf{I}_{N\times N} \end{bmatrix}. \tag{2}$$

The commonly used constrained filter update equation in frequency domain is given by [2]

$$\mathbf{w}_f(k+1) = \mathbf{w}_f(k) + \mathbf{F}\mathbf{G}_{N,0}\mathbf{F}^{-1}\mu\mathbf{M}_f\mathbf{X}_f^{\mathrm{H}}(k)\mathbf{e}_f(k) \tag{3}$$

where the superscript H represents the conjugate transpose operation, μ is a constant step size, $\mathbf{M}_f = \mathrm{diag}[\boldsymbol{\xi}]$ is a diagonal matrix with $\boldsymbol{\xi}$ representing the vector containing the normalizing factors for each frequency bin, and

$$\mathbf{G}_{N,0} = \begin{bmatrix} \mathbf{I}_{N\times N} & \mathbf{0}_{N\times N} \\ \mathbf{0}_{N\times N} & \mathbf{0}_{N\times N} \end{bmatrix}. \tag{4}$$

To accelerate the convergence speed, the normalizing factors in $\mathbf{M}_f$ can be set as the reciprocal of the reference signal power spectrum as

$$\mathbf{M}_f = \mathrm{diag}\left\{\left[\frac{1}{P_0}, \frac{1}{P_1}, \ldots, \frac{1}{P_{2N-1}}\right]^{\mathrm{T}}\right\}, \tag{5}$$

where P_i represents the power spectrum of the ith frequency bin, resulting in the normalized FBLMS (NFBLMS) algorithm. Although the NFBLMS algorithm has been proven to be capable of equalizing all modes of convergence modes [1], a deterioration of the steady state behavior has been found for colored reference signal in non-causal circumstances and/or with deficient filter length [9-10]. To solve this problem, the MFBLMS algorithm updates the filter with [11]

$$\mathbf{w}_f(k+1) = \mathbf{w}_f(k) + \mu\mathbf{M}_f\mathbf{F}\mathbf{G}_{N,0}\mathbf{F}^{-1}\mathbf{X}_f^{\mathrm{H}}(k)\mathbf{e}_f(k)\,. \tag{6}$$

where the difference between Eqs. (3) and (6) is the position of the matrix $\mathbf{M}_f$. The MFBLMS algorithm can guarantee optimal steady state performance at the cost one more FFT/IFFT pair [11].

Applying inverse Fourier transformation on both sides of (6) leads to

$$\begin{bmatrix} \mathbf{w}(k+1) \\ \mathbf{w}_{nc}(k+1) \end{bmatrix} = \begin{bmatrix} \mathbf{w}(k) \\ \mathbf{w}_{nc}(k) \end{bmatrix} + \mu \mathbf{M}\mathbf{G}_{N,0}\mathbf{X}(k) \begin{bmatrix} \mathbf{0}_{N\times 1} \\ \mathbf{e}(k) \end{bmatrix}, \tag{7}$$

where $\mathbf{e}(k) = [e(kN), e(kN+1), \ldots, e(kN+N-1)]^{\mathrm{T}}$, $\mathbf{w}_{nc}(k)$ represents the non-causal part of the adaptive filter which does not influence the filtered output.

$$\mathbf{X}(k) = \mathbf{F}^{-1}\mathbf{X}_f^{\mathrm{H}}(k)\mathbf{F} = \begin{bmatrix} \mathbf{X}_1 & \mathbf{X}_2 \\ \mathbf{X}_2 & \mathbf{X}_1 \end{bmatrix} \tag{8}$$

is a circulant matrix whose first row is $\mathbf{x}(k)$, and

$$\mathbf{M} = \mathbf{F}^{-1}\mathbf{M}_f\mathbf{F} = \begin{bmatrix} \mathbf{M}_1 & \mathbf{M}_2 \\ \mathbf{M}_2 & \mathbf{M}_1 \end{bmatrix} \tag{9}$$

is also a circulant matrix. The updating of the causal part of the filter can then be described as

$$\mathbf{w}(k+1) = \mathbf{w}(k) + \mu \mathbf{M}_1\mathbf{X}_2\mathbf{e}(k)\,. \tag{10}$$

Taking expectation on both sides of (10) yields

$$E\left[\mathbf{w}(k+1)\right] = \left[\mathbf{I}_{N\times N} - \mu \mathbf{M}_1\mathbf{R}\right]E\left[\mathbf{w}(k)\right] + \mu \mathbf{M}_1\mathbf{r}\,. \tag{11}$$

The steady state solution is $E[\mathbf{w}_\infty(k)] = \mathbf{R}^{-1}\mathbf{r}$, and obviously, the MFBLMS results in an unconditional convergence to the Wiener solution. From Eq. (11) it can also be seen that the convergence behavior depends on the matrix $\mathbf{M}_1\mathbf{R}$, hence the convergence behavior can be analyzed by investigating the eigenvalue spread of this matrix.

B. General analysis of an ARMA process

This section proves ……… for systems that can be described by minimum phase stable autoregressive moving average (ARMA) models. The signals can be generated by passing a unit-variance white noise through a pole-zero transfer function

$$H(z) = \frac{\sigma^2 \prod_{i=0}^{Q}\left(z - q_i\right)}{\prod_{i=0}^{P}\left(z - p_i\right)} \tag{12}$$

where σ^2 represents the variance of the signal, p_i and q_i denote the pole and zero of the transfer function respectively. Note that the modulus of both p_i and q_i are smaller than 1. The autocorrelation sequence of this ARMA process is dominated by damped exponentials (from the real poles) and/or damped sine waves (from the conjugate complex poles) [13], thus it is reasonable to assume that the autocorrelation of the reference signal is a sequence of

$$\mathbf{r}_x = \left\{ r_{m,} r_{m-1}, \cdots, r_1, r_0, r_1, r_2, \cdots, r_m \right\}, \tag{13}$$

and $r_i = 0$ for $|i| > m$, so that for a sufficiently large $N > m$, the autocorrelation matrix is banded as [12]

$$\mathbf{R}_x = \text{toeplitz}\left\{ \left[r_0, r_1, \cdots, r_m, \mathbf{0}_{1\times(N-m-1)} \right]^{\mathrm{T}} \right\} \tag{14}$$

where toeplitz{**r**} stands for a symmetric Toeplitz matrix having **r** as its first column.

The Fourier transform of the autocorrelation sequence $\mathbf{r}_x$ is the power spectrum of the reference signal

$$P_x(\omega) = \sum_{k=-m}^{m} r_x(k) e^{-jk\omega} \tag{15}$$

while the reciprocal of $P_x(\omega)$ is the power spectrum of the ARMA process with the transfer function of $1/H(z)$. The transfer function of this inverse ARMA process is also minimum-phase stable, and its autocorrelation sequence can also be assumed as

$$\bar{\mathbf{r}} = \left\{ \bar{r}_{\bar{m},} \bar{r}_{\bar{m}-1}, \cdots, \bar{r}_1, \bar{r}_0, \bar{r}_1, \bar{r}_2, \cdots, \bar{r}_{\bar{m}} \right\}, \tag{16}$$

and $\bar{r}_i = 0$ for $|i| > \bar{m}$, so that for a sufficiently large $N > \bar{m}$, the autocorrelation matrix of this ARMA process is also banded as

$$\bar{\mathbf{R}}_x = \text{toeplitz}\left\{ \left[\bar{r}_0, \bar{r}_1, \cdots, \bar{r}_{\bar{m}}, \mathbf{0}_{1\times(N-\bar{m}-1)} \right]^{\mathrm{T}} \right\}. \tag{17}$$

When the normalizing factor is set proportional to the reciprocal of $P_x(\omega)$ as shown in (5), from the definition of (9), the matrix **M** can be described as

$$\mathbf{M} = \text{circulant}\left\{ \left[\bar{r}_0, \bar{r}_1, \cdots, \bar{r}_{\bar{m}}, \mathbf{0}_{1\times(2N-2\bar{m})}, \bar{r}_{\bar{m}}, \bar{r}_{\bar{m}-1}, \cdots, \bar{r}_1 \right]^{\mathrm{T}} \right\} \tag{18}$$

where circulant{**r**} stands for a circulant matrix having **r** as its first column. From (9), (17) and (18) it can be found that

$$\mathbf{M}_1 = \bar{\mathbf{R}}_x. \tag{19}$$

It has been proven that the Toeplitz matrix of (14) is asymptotically equivalent to a circulant matrix as [12]

$$\mathbf{C} = \text{circulant}\left\{ \left[r_0, r_1, \cdots, r_m, \mathbf{0}_{1\times(N-2m)}, r_m, r_{m-1}, \cdots, r_1 \right]^{\mathrm{T}} \right\}. \tag{20}$$

As described in [12], this asymptotic equivalence is abbreviated as $\mathbf{R}_x \sim \mathbf{C}$. Moreover, from the properties of the asymptotic equivalence matrices as shown in [12],

$$\mathbf{R}_x^{-1} \sim \mathbf{C}^{-1} \tag{21}$$

if the norm of $\mathbf{R}_x^{-1}$ and $\mathbf{C}^{-1}$ are both bounded for any N.

The matrix $\mathbf{C}$ can be decomposed as

$$\mathbf{C} = \mathbf{F}_N^{-1}\mathbf{P}_N\mathbf{F}_N \tag{22}$$

where $\mathbf{F}_N$ represents a $N\times N$ DFT matrix and

$$\mathbf{P}_N = \mathrm{diag}\left\{\mathbf{F}\left[r_0, r_1, \cdots, r_m, \mathbf{0}_{1\times(N-2m)}, r_m, r_{m-1}, \cdots, r_1\right]^{\mathrm{T}}\right\} \tag{23}$$

is a diagonal matrix whose diagonal elements are the power spectra of the reference signal. It is straightforward to find out that

$$\begin{aligned}\mathbf{C}^{-1} &= \mathbf{F}_N^{-1}\mathbf{P}_N^{-1}\mathbf{F}_N \\ &= \mathrm{circulant}\left\{\left[\bar{r}_0, \bar{r}_1, \cdots, \bar{r}_{\bar{m}}, \mathbf{0}_{1\times(N-2\bar{m})}, \bar{r}_{\bar{m}}, \bar{r}_{\bar{m}-1}, \cdots, \bar{r}_1\right]^{\mathrm{T}}\right\}.\end{aligned} \tag{24}$$

Comparing (17) with (24), it can be found that

$$\mathbf{C}^{-1} \sim \bar{\mathbf{R}}_x . \tag{25}$$

Then from (19), (21) and (25), it can be found that

$$\mathbf{M}_1 \sim \mathbf{R}_x^{-1} . \tag{26}$$

Note that $\mathbf{R} = N\mathbf{R}_x$, so that

$$\mathbf{M}_1\mathbf{R} \sim N\mathbf{I}_{N\times N} . \tag{27}$$

Eq. (27) shows clearly that the eigenvalues of the matrix $\mathbf{M}_1\mathbf{R}$ has the tendency to be equally distributed as that of an identity matrix, and this is the reason for the good convergence behavior of the proposed algorithm. However, as pointed out in [12], the result is rather general and does not indicate anything about the convergence of the individual eigenvalues. It is possible that although most of the eigenvalues converge to N, some higher or lower eigenvalues still exist. Thus further assumption about the reference signal is needed to obtain stronger results.

C. Theoretical eigenvalue spread with the first-order AR models

The first-order AR (AR-1) signals are equivalent to the first-order Markov signals, and they are general and practical signals that have often been used in the analysis of adaptive algorithms. The normally used autocorrelation matrix of the AR-1 signals is

$$\mathbf{R}_x = \begin{bmatrix} 1 & \rho & \rho^2 & \cdots & \rho^{N-1} \\ \rho & 1 & \rho & \cdots & \rho^{N-2} \\ \rho^2 & \rho & 1 & & \\ \vdots & \vdots & & \ddots & \vdots \\ \rho^{N-1} & \rho^{N-2} & \cdots & \rho & 1 \end{bmatrix} \tag{28}$$

where $|\rho| < 1$ is the pole of the system. The Z-transform of this autocorrelation sequence is

$$P_x(z) = \sum_{i=-\infty}^{+\infty} \rho^{|i|} z^{-i} = \frac{1-\rho^2}{\left(1-\rho z^{-1}\right)\left(1-\rho z\right)} \tag{29}$$

and the power spectrum of the corresponding signal is

$$P_x(\omega) = \frac{1-\rho^2}{1-2\rho\cos\omega+\rho^2}\,. \tag{30}$$

where ω is the … The eigenvalues of $\mathbf{R}_x$ can be analytically expressed as [14]

$$\lambda_i = \frac{1-\rho^2}{1-2\rho\cos\gamma_i+\rho^2},\ i = 0,1,\cdots,N-1 \tag{31}$$

where $0 < \gamma_0 < \pi/(N+1) < \gamma_1 < 2\pi/(N+1) < \gamma_2 < \ldots < \gamma_{N-1} < N\pi/(N+1)$, and N is a large number for highly correlated signals. The eigenvalue spread of the matrix $\mathbf{R}_x$ controls the convergence behaviour of the time domain LMS algorithm, and it approaches $(1+|\rho|)^2/(1-|\rho|)^2$ when N is sufficiently large.

The reciprocal of the power spectrum of (30) corresponds to an autocorrelation sequence whose Z-transform is $(1-\rho z^{-1})(1-\rho z)/(1-\rho^2)$. Accordingly, the autocorrelation sequence is

$$\bar{r}_i = \begin{cases} \dfrac{1+\rho^2}{1-\rho^2},\ i=0 \\ \dfrac{-\rho}{1-\rho^2},\ i=-1 \text{ or } 1\,. \\ 0,\ \text{else} \end{cases} \tag{32}$$

Thus when the normalizing factor is set as (5),

$$\mathbf{M}_1 = \frac{1}{1\text{-}\rho^2}\begin{bmatrix} 1+\rho^2 & -\rho & 0 & \cdots & 0 \\ -\rho & 1+\rho^2 & -\rho & \ddots & \vdots \\ 0 & -\rho & 1+\rho^2 & \ddots & 0 \\ \vdots & \ddots & \ddots & \ddots & -\rho \\ 0 & \cdots & 0 & -\rho & 1+\rho^2 \end{bmatrix} \tag{33}$$

Note that (33) is the same as the analytical inverse of the autocorrelation matrix (28) as depicted in [15] except the first element of the first row and the last element of the last row.

Multiplying (28) and (33) yields

$$\mathbf{M}_1\mathbf{R}_x = \frac{1}{1\text{-}\rho^2}\begin{bmatrix} 1 & \rho^3 & \rho^4 & \cdots & \rho^{N+1} \\ 0 & 1\text{-}\rho^2 & 0 & \ddots & 0 \\ \vdots & \ddots & \ddots & \ddots & \vdots \\ 0 & \ddots & 0 & 1\text{-}\rho^2 & 0 \\ \rho^{N+1} & \cdots & \rho^4 & \rho^3 & 1 \end{bmatrix} . \tag{34}$$

Applying the Girschgorin Circle theorem [16] to the middle N-2 rows of the matrix in (34), it can be deduced that N-2 eigenvalues of $\mathbf{M}_1\mathbf{R}_x$ are equal to 1. Denote the rest 2 eigenvalues as λ_0 and λ_1, then from the definition of the trace of the matrix in (34), it can be found that

$$\lambda_0 + \lambda_1 = \frac{2}{1-\rho^2} . \tag{35}$$

On the other hand, the matrix (34) can be transformed to an upper triangular matrix by adding scalar multiples of the last column to the first N-1 columns, so that the determinant is

$$\det\left(\mathbf{M}_1\mathbf{R}_x\right) = \lambda_0\lambda_1 = \frac{1-\rho^{2(N+1)}}{1-\rho^2} . \tag{36}$$

From (35) and (36), the rest 2 eigenvalues of the matrix (34) can be calculated out as $\lambda_0 = (1+\rho^{N+1})/(1\text{-}\rho^2)$ and $\lambda_1 = (1\text{-}\rho^{N+1})/(1\text{-}\rho^2)$. Both of these two eigenvalues approach $1/(1\text{-}\rho^2)$ for sufficiently large N, leading to a eigenvalue spread of $1/(1\text{-}\rho^2)$ significantly smaller than that of $\mathbf{R}_x$ especially when the signal is highly correlated. Note that $\mathbf{R} = N\mathbf{R}_x$, so that the eigenvalue spread of $\mathbf{M}_1\mathbf{R}$ is the same as that of $\mathbf{M}_1\mathbf{R}_x$. Interestingly, this eigenvalue spread happens to be the same as that of the transform domain LMS algorithm using the … (DST), which is proven to be the best among all the transform domain algorithms for AR-1 signals [17]. Considering the computational efficiency, the MFBLMS algorithm is a better option for steady state performance critical implementations.

Few general comments based on theoretical analyses, comparisons and discussion with the existing algorithms such as NFBLMS and TDLMS … …. advantages and disadvantages

III. SIMULATIONS

The eigenvalues of the matrix controlling the convergence of the NFBLMS algorithm has been proven to be equally distribution in [1]. From the above analysis, although the eigenvalue distribution of the matrix controlling the convergence of the MFBLMS algorithm is not as ideal as that of the NFBLMS algorithm, it is significantly better than that of the time domain LMS algorithm (abbreviated as TDLMS hereafter) for colored reference signals. Several simulations are given in this section to validate the theoretical analysis. The step sizes for all the following simulations are carefully chosen close to the upper limits to guarantee both the fastest convergence speed and stable steady state behaviors, and all the results are averaged over 200 independent trials.

A. Deficient filer-length case for AR-1 reference signals

In this simulations, the reference signals were generated by passing Gaussian white noise with unit variance through two transfer functions $H_1(z) = 1/(1\text{-}0.9z^{-1})$ and $H_2(z) = 1/(1\text{-}0.99z^{-1})$, leading to AR-1 models with the correlation parameter $\rho = 0.9$ and $\rho = 0.99$ respectively. The desired signal was generated by passing the reference signal through a 128-tap bandpass filter with passband of $[0.2\pi, 0.5\pi]$. A 100-tap FIR filter was utilized, resulting in a typical deficient filter length case. The eigenvalue spread of these two AR-1 models for different algorithms are shown in Table 1. It can be found that the eigenvalue spread of both the NFBLMS algorithm and the MFBLMS algorithm are much lower than that of the TDLMS algorithm, and the difference increases with the growth of the correlation parameter of the model. This coincides with the analysis in Sec. II.C. The filter length 100 is sufficiently large for the AR-1 signal with $\rho = 0.9$, and the eigenvalue spread shown in Table 1 is exactly the same as the analytical result $1/(1\text{-}\rho^2) = 5.3$. For the AR-1 signal with $\rho = 0.99$, the eigenvalue shown in Table 1 is smaller than the analytical result $1/(1\text{-}\rho^2) = 50.2$ since the filter length 100 is not sufficiently large in this case. However, it is found that with the increase of the filter length, the eigenvalue spread approaches the analytical result.

From the convergence behavior of different algorithms depicted in Fig. 1, it can be seen that the NFBLMS algorithm converges fastest but to a biased solution. The MFBLMS algorithm converges slower than the NFBLMS algorithm but significantly faster than the TDLMS algorithm. It can also be seen that when the correlation parameter increases from 0.9 to 0.99, the convergence speed of all the algorithms reduces considerably (note the difference of the total samples in Fig. 1(a) and 1(b)), and the difference of the convergence behavior between the algorithms increases drastically, which can be well explained by the eigenvalue spread shown in Table 1.

Table 1. Eigenvalue spread of the AR-1 models with 100 filter taps

	NFBLMS	MFBLMS	TDLMS
ρ = 0.9	1.1	5.3	339.5
ρ = 0.99	1.8	43.5	14678.9

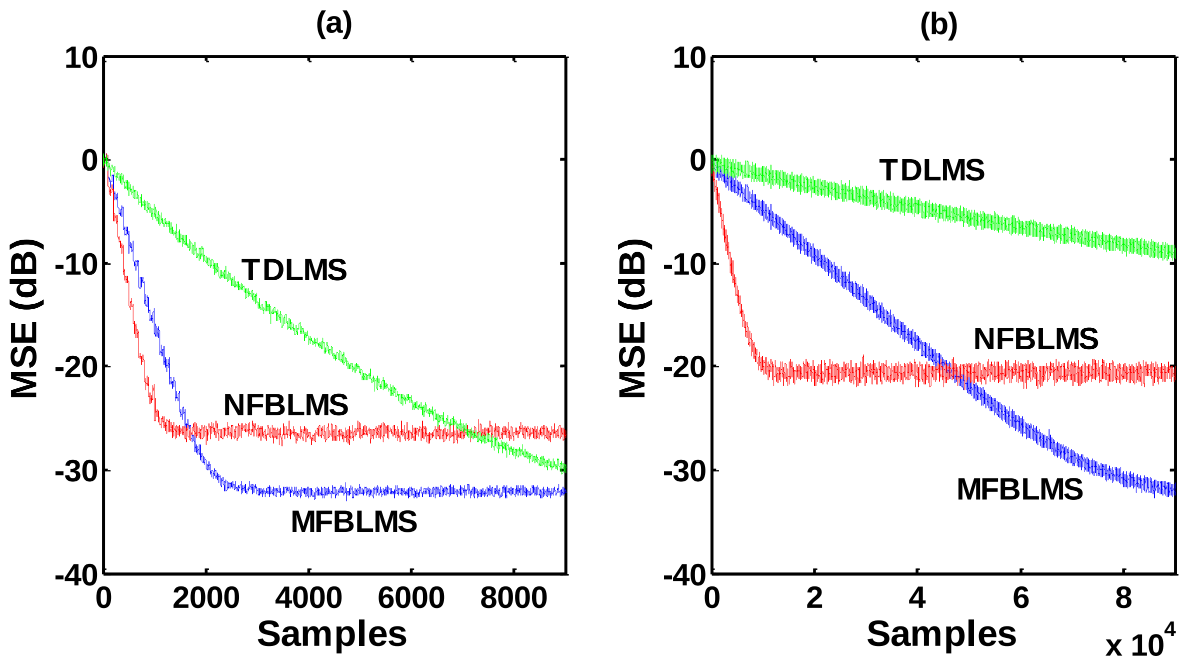

Fig 1. Convergence behavior of the AR-1 signals with (a) ρ = 0.9 and (b) ρ = 0.99 under deficient filter length conditions.

B. Deficient filer-length case for ARMA reference signals

In this simulation, the reference signal was generated by passing Gaussian white noise with unit variance through a low pass filter with an ARMA transfer function $H(z) = [(1-0.5z^{-1})/(1-0.6z^{-1})]^{16}$. The desired signal was generated by passing the reference signal through the same bandpass filter as that in Sec. III.A, and the filter length was still 100. The eigenvalue spread of this ARMA model for different algorithms are shown in Table 2. It can be found that the eigenvalue spread of the MFBLMS algorithm is still much lower than that of the TDLMS algorithm. Further investigation shows that except two large eigenvalues, nearly all the eigenvalues of the matrix $\mathbf{M}_1\mathbf{R}_x$ controlling the convergence behavior of the MFBLMS algorithm are very close to 100, which coincides with the analysis in Sec. II.B.

The convergence behavior of different algorithms for this ARMA signal is shown in Fig. 2. It can be seen that the NFBLMS algorithm converges very fast but to a biased solution. Although the MFBLMS algorithm converges slower than the MFBLMS algorithm, it has a much lower steady-state MSE, and its convergence speed is significantly faster than that of the TDLMS algorithm, which is consistent with the eigenvalue spread shown in Table 2.

Table 2. Eigenvalue spread of an ARMA model with 100 filter taps

NFBLMS	MFBLMS	TDLMS
2.7	108.3	9932.9

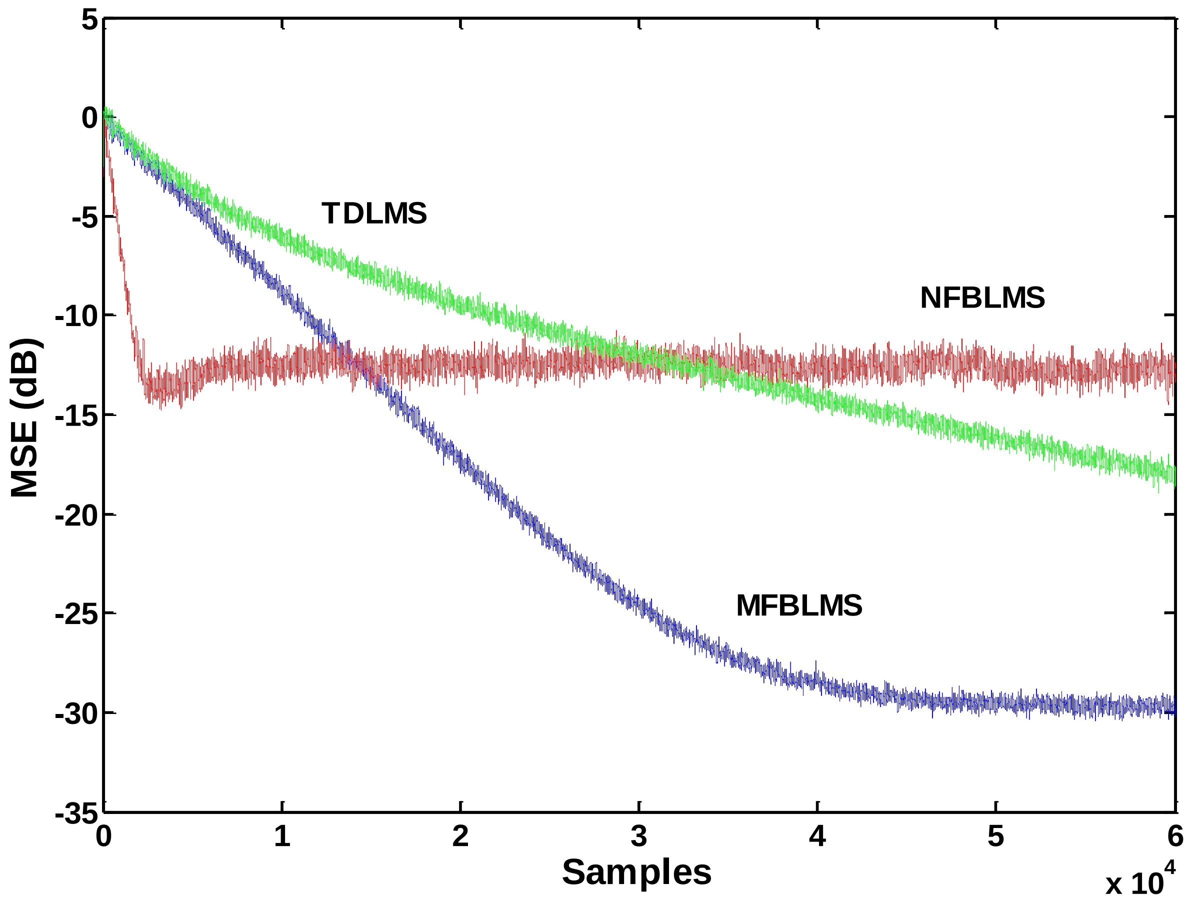

Fig. 2. Convergence behavior of the ARMA signals under deficient filter length conditions.

C. Non-causal case

In this simulation, two reference signals were utilized. One is the same as that used in Sec. III.A with $\rho = 0.99$ and the other is the same as that used in Sec. III.B. The desired signal was one sample ahead of the reference signal, resulting in a typical non-causal linear prediction problem. The adaptive filter length N was still 100. The convergence behavior of different algorithms is shown in Fig. 3. As expected, the MFBLMS algorithm converges slower than the NFBLMS algorithm but to a much lower steady-state MSE. The TDLMS algorithm converges very fast initially, then the slow modes dominate, leading to a significantly slower convergence speed than that of the MFBLMS algorithm.

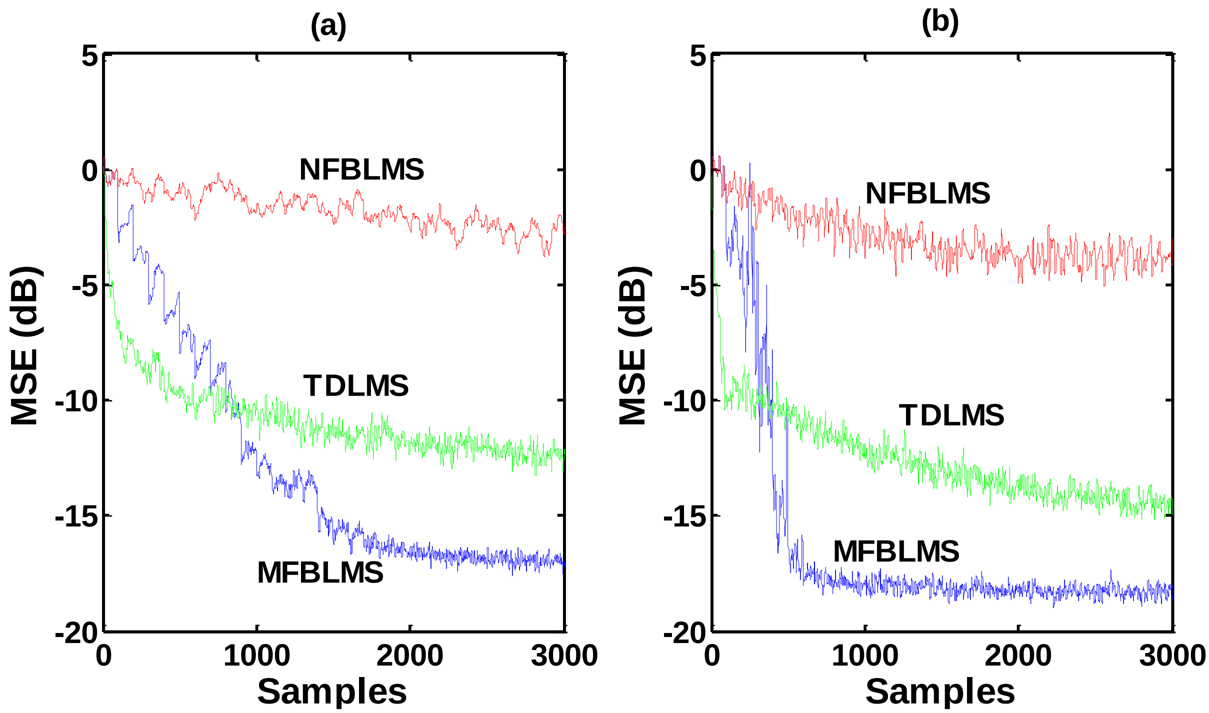

Fig. 3. Convergence behavior under non-causal conditions with reference signals of (a) AR-1 model (b) ARMA model.

These simulations clearly validate the theoretical analysis of the convergence behavior. Although the convergence speed of the MFBLMS algorithm is not as good as that of the NFBLMS algorithm, but significantly better than the TDLMS algorithm because the eigenvalue disparity of the matrix controlling the convergence of the MFBLMS algorithm is considerably better than that of the TDLMS algorithm.

IV. Conclusion

The convergence behavior of the MFBLMS algorithm is investigated by using the theory of asymptotical equivalent matrices, and it shows that the eigenvalues of the proposed algorithm have the tendency to be equally distributed as that of an identity matrix. Further analysis of the eigenvalue spread based on the first-order AR model proves that the eigenvalue spread of the MFBLMS algorithm is significantly lower than that of the TDLMS one. The theoretical analysis results are supported by numerical simulations. With these analyses, it can now be safely concluded that the MFBLMS algorithm does have the benefits of both lower computational complexity and faster convergence speed than the time domain algorithm, while effectively overcome the problem of biased steady-state solution of the NFBLMS algorithm.

REFERENCES

[1] B. Farhang-Boroujeny, *Adaptive Filters: Theory and Applications*. Chichester, U.K.: Wiley, 1998.

[2] J. J. Shynk, "Frequency-domain and multirate adaptive filtering," *IEEE Signal Processing Mag.*, pp. 14–37, Jan. 1992.

[3] K. Shi and X. L. Ma, "A frequency domain step-size control method for LMS algorithms", *IEEE Signal Processing Letters*, vol. 17, no. 2, pp. 125-128, 2010.

[4] J. Lee and H. C. Huang, "On the step-size bounds of frequency-domain block LMS adaptive filters", *IEEE Signal Processing Letters*, vol. 20, no. 1, pp. 23-26, 2013.

[5] M. Wu and J. Yang, "A step size control method for deficient length FBLMS algorithm", *IEEE Signal Processing Letters*, vol. 22, no. 9, pp. 1448-1451, 2015.

[6] M. Wu, G. Chen, and X. Qiu, "An improved active noise control algorithm without secondary path identification based on the frequency-domain subband architecture," *IEEE Trans. Audio, Speech, Lang. Process.*, vol. 16, no. 8, pp. 1409–1419, Oct. 2008.

[7] S. Wu, X. J. Qiu and M. Wu, "Stereo acoustic echo cancellation employing frequency-domain preprocessing and adaptive filter", *IEEE Trans. Audio, Speech, Lang. Process.*, vol. 19, no. 3, pp. 614-623, Mar. 2011.

[8] Y. T. Huang and J. Benesty, "A class of frequency-domain adaptive approaches to blind multichannel identification", *IEEE Trans. Signal Process.*, vol. 51, no. 1, pp. 11-24, Jan. 2003.

[9] S. J. Elliott and B. Rafaely, "Frequency-domain adaptation of causal digital filters," *IEEE Trans. Signal Process.*, vol. 48, no. 5, pp. 1354-1364, May 2000.

[10] M. Wu, J. Yang, Y. Xu, and X. J. Qiu, "Steady-state solution of the deficient length constrained FBLMS algorithm", *IEEE Trans. Signal Process.* vol. 60, pp. 6681-6687, Dec. 2012.

[11] J. Lu, X. J. Qiu, and H. S. Zou, "A modified frequency-domain block LMS algorithm with guaranteed optimal steady-state performance", *Signal Processing*, 104, 27-32, 2014.

[12] R. M. Gray, “Toeplitz and circulant matrices: A review,” *Found. Trends. Commun. Inform. Theory*, vol. 2, no. 3, pp. 155–239, 2006.

[13] D. G. Manolakis, V. K. Ingle and S. M. Kogon, *Statistical and Adaptive Signal Processing: Spectral Estimation, Signal Modeling, Adaptive Filtering and Array Processing*, Boston, MA: McGraw-Hill, 2000.

[14] M. Dow, “Explicit inverses of Toeplitz and associated matrices,” *Australian/New Zealand Ind. Appl. Math. J.*, vol. 44, no. E, pp. 185–215, Jan. 2003.

[15] W. F. Trench, “Numerical solution of the eigenvalue problem for Hermitian Toeplitz matrices”, *SIAM J. Matrix Anal. Appl.* vol. 10, pp. 135-156, 1989.

[16] C. D. Meyer, *Matrix Analysis and Applied Linear Algebra*. Philadelphia, PA: SIAM, 2000.

[17] S. K. Zhao, Z. H. Man, S. Y. Khoo, and H. R. Wu, “Stability and convergence analysis of transform-domain LMS adaptive filters with second-order autoregressive process,” *IEEE Trans. Signal Process.*, vol. 57, no. 1, pp. 119–130, Jan. 2009.